Drug Discovery Today

MRI Assessment of Cerebral Perfusion in Clinical Trials

--Manuscript Draft--

Manuscript Number:	
Article Type:	SI: Reviews 2022 – part II
Keywords:	Arterial spin labeling-MRI, cerebral perfusion, clinical trial, multicenter trials
Corresponding Author:	lino becerra Invicro LLC UNITED STATES
First Author:	lino becerra
Order of Authors:	lino becerra
	Xue Wang
	Courtney Bishop
	James O'Callaghan
	Justin Albani
	Wendy Theriault
	Michael Chappell
	Xavier Golay
	Danny Wang
Abstract:	Neurodegenerative mechanisms affect the brain through a variety of processes that are reflected as changes in brain structure and physiology. While some biomarkers for these changes are well established, others are at different stages of development for use in clinical trials. One of the most challenging biomarkers to harmonize for clinical trials is cerebral blood flow. There are a number of MRI methods for quantifying CBF without the use of contrast agents, in particular Arterial Spin Labeling (ASL) perfusion MRI which has been increasingly applied for clinical trials. In this review, we present ASL MRI techniques, including strategies for implementation across multiple imaging centers, levels of confidence in assessing disease progression and treatment effects, and details of image analysis.
Suggested Reviewers:	Ona Wu, PhD Assoc Prof, Harvard University ona.wu@mgh.harvard.edu Expert in perfusion imaging
	Peter Hardy, PhD Assoc Professor, University of Kentucky College of Medicine Peter.Hardy@uky.edu Expert in MRI and physiology

Highlights

This article provides an up-to-date review of the use and applications of arterial spin labeling, an MRI modality to assess perfusion without the use of exogeneous contrast agents. Their utility has become more prevalent in clinical trials as expressed, it does not require exogeneous contrast agents and may complement PET studies as a potential replacement for 18F FDG scans.
The article describes the following:

- Use of MRI perfusion imaging in clinical trials
- Detailed description of procedures, best practices in clinical trials
- Review of currently available software and recommendations
- Assessment of test re-test repeatability of ASL
- Compiled references for further detailed description of the technique, applications beyond neuroimaging.

MRI Assessment of Cerebral Perfusion in Clinical Trials

Authors:
Xue Wang[1]*, Courtney Bishop[1]*, James O'Callaghan[1], Justin Albani[1], Wendy Theriault[1], Michael Chappell[2], Xavier Golay[3], Danny Wang[4], Lino Becerra[1]

Author addresses:

1. Invicro, LLC
   Needham, Massachusetts
2. Radiological Sciences, Mental Health & Clinical Neurosciences, School of Medicine
   Sir Peter Mansfield Imaging Centre, School of Medicine
   University of Nottingham
3. Brain Repair & Rehabilitation
   UCL Queen Square Institute of Neurology
   University College London
4. Laboratory of FMRI Technology (LOFT)
   Mark & Mary Stevens Neuroimaging and Informatics Institute
   Keck School of Medicine
   University of Southern California (USC)

*Contributed equally
Corresponding Author: Lino Becerra lbecerra@invicro.com

Key words (≤ 6): Arterial spin labeling-MRI, cerebral perfusion, clinical trial, multicenter trials

Teaser: This review provides an overview of the implementation of ASL MRI in clinical trials for the assessment of cerebral blood flow.

Statement

This article provides an up-to-date review of the use and applications of arterial spin labeling, an MRI modality to assess perfusion without the use of exogeneous contrast agents. Their utility has become more prevalent in clinical trials as expressed, it does not require exogeneous contrast agents and may complement PET studies as a potential replacement for 18F FDG scans.
The article describes the following:

- Use of MRI perfusion imaging in clinical trials
- Detailed description of procedures, best practices in clinical trials
- Review of currently available software and recommendations
- Assessment of test re-test repeatability of ASL
- Compiled references for further detailed description of the technique, applications beyond neuroimaging.

Authors

Xue Wang PhD

Xue Wang is a Senior Scientist at Invicro, a leading medical imaging service provider located in Boston. In this role, she supports application of imaging in clinical trials for biopharmaceutical partners across all phases of drug development (preclinical through registrational studies). Prior to this role, she was a research faculty at the Center for Translational Imaging at the Department of Radiology at Northwestern University Chicago. Here she pursued clinical research leveraging imaging to investigate brain structural and function changes associated with neurorehabilitative treatment in various neurological disorders. Xue Wang has a doctorate in biomedical engineering.

Courtney Bishop PhD

Courtney Bishop was formerly a Senior MRI Scientist at Invicro London, leading the application of multi-parametric, quantitative clinical MRI studies for academia and industry sponsors with particular emphasis on delivering appropriate study designs and analytics. Courtney is Senior Imaging Technology Leader for MRI at GE Healthcare, leading the imaging strategy for clinical development of novel MRI perfusion-imaging agents. Of particular relevance to this work: Courtney is highly experienced (>10 years) in ASL imaging and analysis, having been MR lead on a number of single- and multi-site clinical studies utilising MRI to examine brain changes in response to either aging, disease, or drug interventions.

Lino Becerra PhD

Lino Becerra is Vice President for MRI at Invicro, a leading imaging service provider where he oversees MR operations from pre-clinical studies to late clinical trials. He is an MRI physicist by training and leads the implementation and execution of multisite multimodal clinical trials as well as the development and deployment of analytical tools. He has over 25 years of experience in neuroimaging in academia and industry having been the co-Director for the Center for Pain and the Brain at Harvard as well as an Associate Professor. Dr. Becerra has co-authored over 180 publications in leading journals. He is the Vice President for MRI at Invicro

Abstract

Neurodegenerative mechanisms affect the brain through a variety of processes that are reflected as changes in brain structure and physiology. While some biomarkers for these changes are well established, others are at different stages of development for use in clinical trials. One of the most challenging biomarkers to harmonize for clinical trials is cerebral blood flow. There are a number of MRI methods for quantifying CBF without the use of contrast agents, in particular Arterial Spin Labeling (ASL) perfusion MRI which has been increasingly applied for clinical trials. In this review, we present ASL MRI techniques, including strategies for implementation across multiple imaging centers, levels of confidence in assessing disease progression and treatment effects, and details of image analysis.

Introduction

Adequate cerebral blood flow (CBF) plays a critical role in maintaining the brain's structural and functional integrity, as it provides a constant supply of oxygenated blood and nutrients [1]. In several neurological disease conditions, reduced brain perfusion and metabolism is commonly observed. There is an association between brain atrophy and reduced CBF, and studies indicate that reduced flow may result in brain atrophy [2]. For example, in Alzheimer's Disease, patients display hypoperfusion/hypometabolism most markedly in the temporoparietal lobe and posterior cingulate cortex, precuneus and frontal cortex [3], and in Parkinson's Disease, patients present hypoperfusion in posterior parieto-occipital structures [4]. Furthermore, cardiovascular disease is linked to reduced brain perfusion and subsequent neurodegeneration [5].

The re-establishment of perfusion seems to aid in the alleviation of the symptoms in the case of neurodegeneration associated with cardiovascular dysfunction and could contribute to slowing cognitive impairment [5]. In acute stroke, perfusion measurement is critical for assessing compromised tissue, aiding treatment decisions for interval therapy to re-establish circulation, determining collateral perfusion, and predicting clinical outcome [6, 7]. The evaluation of brain perfusion is therefore relevant for the assessment of disease states as well as disease modifying treatments.

Arterial Spin Labeling is a non-invasive magnetic resonance imaging (MRI) technique that is an ideal tool to study brain perfusion over time. ASL does not require radioactive or exogenous contrast agents, and it provides a relatively reproducible quantitative CBF measurement [8]. A review of open clinical trials (EU Clinical Trials Register, clinicaltrials.gov) revealed several studies assessing blood flow in a variety of conditions, including cognitive impairment, multiple sclerosis, oncology, and stroke.

In this review, we provide the reader with an understanding of the ASL technique and guidance on the operational aspects of implementation and image analysis, focusing on neurodegeneration-related clinical trials. For other clinical applications as well as for perfusion assessment of other organs such as kidney or heart, the reader is referred to the literature [9-11].

This review encompasses the following sections: an introduction of the technique, the applications of ASL imaging followed by the procedures for imaging site setup, qualification, patient preparation as well as the imaging data quality control, analysis, and storage.

Arterial Spin Labeling

ASL is an MRI-based perfusion imaging technique that can quantitatively measure microvascular blood flow or perfusion, as well as other hemodynamic parameters such as arterial blood volume, and arterial transit time [12-14]. In 1992, Williams et al. proposed the original ASL method, applied to measure CBF of rat brain [13], and in 1994, Detre et al. extended the application to measure human brain perfusion [15]. Tissue perfusion measured by ASL assesses the rate of delivery of nutrients, including oxygen, through blood flow in the capillary beds, which is different from macrovascular blood flow in arteries and veins that can be assessed with other MRI approaches such as MRI Angiography. In particular, using ASL, arterial water spins are labelled and followed until they exchange with the surrounding tissue, where they alter the apparent T1 of the tissue. Various imaging techniques have been developed to measure regional cerebral perfusion in addition to ASL, including positron emission tomography (PET), single photon emission computed tomography (SPECT), Xenon-enhanced computed tomography (CT), dynamic susceptibility contrast MRI (DSC-MR), and Doppler ultrasound (see **Box 1**). ASL is commonly compared with ^{18}F-fluorodeoxyglucose (FDG) PET, although these techniques measure different physiological parameters: blood flow (ASL) vs. rate of glucose consumption (FDG PET). However, brain perfusion and metabolism are tightly coupled under normal conditions, and ASL measured perfusion has shown good correlation with metabolism measured by FDG PET. Additionally, ASL has been used to study brain perfusion/metabolism in place of or in addition to FDG PET [16-18].

Compared to other imaging techniques, ASL MRI has the following advantages: requires no exogenous agent (radioactive or not) nor radiation; has whole brain coverage with a relatively high spatial resolution (2-4 mm) in 5-10 min; and requires no waiting time between two successive exams (for a review see Wintermark 2005 [19]). The main limitations of ASL are the following: ASL has a relatively low signal-to-noise ratio (SNR); ASL is susceptible to head motion; and there are a large variety of ASL sequences and analysis methodologies, which makes protocol harmonization and analysis across imaging sites challenging to implement and compare. However, given its wide availability and relative advantages, a community consensus was

developed in 2015, and has since played and will continue to play an important role for standardized ASL acquisition and analysis across MR platforms and sites [20].

ASL Mechanism and Approaches

ASL takes advantage of an endogenous contrast agent (blood) to determine cerebral blood flow (for a review of ASL imaging see (**Figure 1**) [21]). In the preparation (or labeling) phase, blood water protons outside of the imaging volume are labeled by magnetic inversion (negative magnetization). After a period of time, generally referred to as the 'inflow time' (but more specifically defined as the 'inversion time' (TI) or 'post labelling delay' (PLD) depending on the particular ASL technique being used, there are single PLD and multi-PLD sequences), the image acquisition commences. The inflow time is long enough so that the labeled blood water flows into the imaging tissue and mixes with the (positively magnetized) static tissue water in the parenchyma. The time takes for the labelled blood to reach the vascular or tissue is termed arterial transit time. The long inflow time also allows the much more rapid vascular flow to enter and leave the imaged tissue before it is imaged. Once the labeled blood enters, it produces a net reduction of the parenchymal MRI signal in this 'labeled' image through exchange at the capillary level. A relative measure of perfusion can be calculated by acquiring an unlabeled (control) image and calculating the signal difference between the control and labeled images. The difference in intensity can be converted to CBF based on specific model of tracer kinetics. This perfusion-related signal reduction is small in magnitude, approximately 1-2% of the tissue signal intensity and is very sensitive to the conditions under which the signal is sampled. It is affected by tissue properties such as the blood flow rate and T1 relaxation of blood and parenchymal tissue, as well as factors driven by the selection of MRI equipment and pulse sequence used for acquisition. Background suppression techniques are utilized to selectively minimize the static tissue signal from the rest of the brain to boost the signal-to-noise ratio (SNR) in ASL signal [22].

As illustrated in **Figure 2**, the two most common labeling approaches for ASL are pseudo-continuous ASL (PCASL) and pulsed ASL (PASL). For PCASL labelling, a train of radiofrequency (RF) pulses are applied in rapid succession (over milliseconds) and for a relatively long overall duration (1-3 seconds), to invert and label arterial blood water as it flows through a relatively thin labeling plane. In contrast, PASL typically uses a single RF pulse applied for a much shorter total duration (e.g. 10–20 ms), to simultaneously invert arterial water in a thick labeling slab. For a comment on the resultant SNR differences between PASL and PCASL please see [20], it is generally expected for PCASL to have higher SNR and thus is becoming the sequence of choice. Note that CASL, where one single long continuous ASL label is applied, has lower labeling efficiency compared to PCASL and needs an additional labeling coil. Therefore, it is not recommended for clinical imaging.

ASL readout schemes broadly fall in the category of either 2D or 3D, with a segmented 3D readout (such as 3D multi-echo (RARE) stack-of-spirals [22, 23] or 3D gradient and spin echo (GRASE) [24-

26]). These are the currently recommended default implementations [20] because these readout schemes can be made SNR efficient and are relatively insensitive to off-resonance effects.

The difference between control and labeled ASL scans is a perfusion-weighted image (PWI); to determine absolute perfusion, a separate calibration image (M0) needs to be acquired. This is typically a replication of the ASL 'control' image acquisition but without any background suppression. The process to calculate absolute perfusion from perfusion-weighted images is described in the quantitative analysis section.

ASL Test-retest

Critical to clinical trials, as well as for research and clinical use, an assessment of the degree of reproducibility of CBF measurements utilizing ASL needs to be defined. Many studies have been conducted to evaluate CBF repeatability using different variants of ASL sequences and healthy volunteers, patients, as well as phantoms (see **Table 1** for a summary of these studies). Currently, however, there is no systematic review and meta-analysis of all the test-retest studies in the literature. Nevertheless, overall CBF measurements in GM showed moderate to excellent reliability in Intraclass Correlations (ICC) (0.91>ICC>0.5) in most of these studies, however, there are large variabilities across sites and studies (due to different ASL techniques). In the study by Peterson et al 2010 [29], ICC in GM CBF ranges from 0.07~0.81 across 28 sites (using QUASAR, a sequence not often used). In addition, the degree of reproducibility varied in different brain regions, from ICC=0.91 in the hippocampus to 0.49 in amygdala [27], in disease states, the variability could be larger, for instance, ICC ranges from 0.24~0.75 for patient with FTD in different regions [28]. While most studies focus on CBF, Cohen 2020 [34] also reported the reliability of ATT (ICC range 0.49~0.69), slightly lower than CBF (ICC range 0.66~0.75). The variability across regions and techniques indicates that careful consideration needs to be given when planning a study so that the appropriate statistical power is achieved in the brain regions of interest. In general, a systematic review and meta-analysis of all the test-retest studies should be compiled to establish what are the ICC values in CBF measurement derived from ASL.

Table 1 Summary of ASL test-retest studies

Author (year)	Study population	Interval	site/sequences	ICC for CBF
Petersen et al 2010[29]	284 healthy volunteers	two weeks on average (13±10 days)	28 sites, QUASAR	GM (range: 0.07~0.81 in all sites)

Chen et al. 2011 [27]	12 young healthy subjects	Up to 1 week	Single site, 3T, PCASL, PASL	GM/WM is 0.911/0.877 (PCASL); 0.835/0.825 (PASL)
Kilroy et al. 2014[30]	13 elderly MCI:6, mild AD:1	~ 4 weeks	3D GRASE pCASL, 2D EPI pCASL	0.707 (GRASE pCASL), 0.362 (EPI pCASL) across 24 ROIs
Hodkinson et al 2013[31]	16 healthy male volunteers (age range: 18–50 years)	5 sessions, separated by less than one week or 2-4 weeks	Single site, 3T, PCASL	The inter- and intra-session reliability of the post-surgical pCASL CBF measurements ICC > 0.6, between pre- and post-surgical states ICC > 0.4.
Lin et al 2020 [32]	20 adult volunteers (age 56.6 ± 17.2 years)	1 h	3D pCASL with standard (1500ms) and long (3500ms) delay	precentral cortex (0.84 in left and 0.81 in right)
Jann et al 2021[33]	45 elderly Latinx subjects	~6 weeks	3D pCASL	Whole brain 0.84, WM 0.77,
Cohen et al 2020 [34]	Fifty-two healthy, male subjects	4 sessions over 45 days	3D pCASL with Hadamard-Encoded multiple PLD, (seven PLDs from 1.0–3.7 sec).	ICC CBF (0.75, 0.66,0.72, 0.72 for day 7, 14, 30, 45) ICC ATT (0.69,0.57,0.55,0.49 for day 7, 14, 30, 45)
Ssali et al 2021[28]	13 healthy controls and 8 patients with FTD or progressive supra-nuclear palsy	One month	pCASL	0.5 ~0.8 for control, 0.24~0.75 for patient <0.4 for Amygdala and temporal pole

Binnie et al 2022[35]	54 older adults with small vessel disease (mean age:66.9)	>7 days	Multi site pCASL PASTIS (trial)[36]	GM:0.771, deep GM: 0.872,
Wang et al 2021[37]	3D printed perfusion phantom	One session per week for 5 weeks	2D pCASL with 20 PLDs	ICC=0.96 (95% CI 0.83-1.00)

Image Acquisition

A major challenge in the use of ASL in clinical trials has been the harmonization of image acquisition protocols in multicenter studies [20, 38]. It is likely that sites selected to participate may have MRI systems that differ in manufacturer, field strength, software, and RF coils used to receive signal. While satisfactory ASL imaging can be achieved at 1.5 T, 3 T systems offer greater intrinsic SNR. Furthermore, the lengthening of T1 at higher field strengths provides an additional boost to signal at 3 T as more labeled signal accumulates for a given inflow time. Compensatory reductions in resolution and/or increases in scan time can be made to 1.5 T acquisitions to increase SNR, but introduction of such discrepancies in imaging protocols is undesirable. With regards to RF coil hardware, receiver coils with a greater number of elements will likely offer superior SNR and enable use of parallel imaging methods.

Thankfully, ASL pulse sequences have been implemented by the major MRI scanner vendors and are widely available across their platforms. It has been shown that CBF measurements can be reproducibly produced across vendor platforms when the "identical" pulse sequence is used with parameters as closely matched as possible across platforms [39]. An important recent development is that for every new scanner being sold now, the ASL pulse sequence provided by the main three manufacturers all follow the White Paper recommendations. As such, including sites with novel equipment/ latest SW level might be one way to ensure comparable pulse sequences across the board. However, such approaches may not be feasible in many clinical trials where the imaging corelab may be restricted to deploying commercially available sequences offered by the major MRI vendors in legacy systems as well. At the time of this writing, there remains a lack of standardization, both between vendors and within a vendor's portfolio of scanner models and system software versions. Imaging corelabs are often confronted with a mixture of sequences across trial imaging sites that vary in spin labeling (PASL, CASL, PCASL), readout (EPI, Spiral, GRASE, etc.), and 2D and 3D acquisitions. Furthermore, sequence characteristics that commonly vary between systems include choice of inflow times (and whether to acquire single or multi-delay data), background suppression, acquisition of M0 image, and

achievable resolution. A detailed discussion of ASL implementations is beyond the scope of this paper, but interested readers are directed to existing publications that provide greater technical detail and insight [20, 40, 41].

Finally, ASL readout schemes broadly fall in the category of either 2D or 3D, with a segmented 3D readout (such as 3D multi-echo (RARE) stack-of-spirals [22, 23] or 3D GRASE [24-26], currently recommended as the default implementation [20] because these readout schemes can be made SNR efficient and relatively insensitive to off-resonance effects.

Recommendations

A number of studies have indicated that significant variability can be introduced into ASL studies by departure from consistent scanning equipment, labeling and readout schemes, and protocol parameters [38, 42-44]. Recommendations for pulse sequence deployment are highly dependent upon the ASL endpoints specific to a clinical trial, as well as the number of imaging sites required. When there are a limited number of imaging centers involved, it may be possible to select the sites based on ASL imaging capabilities and limit the sites to those with the same scanning equipment and pulse sequences. When deployment across a variety of scanning equipment and commercial ASL sequences is necessary, it is advised that 3 T scanners be used with RF coils that have an element count greater than or equal to 8. To reduce measurement bias between sites, consistent preparation and acquisition approaches should be used across sites where possible. Pulse sequence parameter guidance for common sequences can be found in the 'Recommended implementation of arterial spin-labeled perfusion MRI for clinical applications' consensus paper published by the ISMRM perfusion study group [20] as well as **Table 2**. Recently, Quantitative Imaging Biomarkers Alliance (QIBA) and European Imaging Biomarkers Alliance (EIBALL) organizations formed a collaborative committee to develop a standardized CBF biomarker calculated from ASL images [45]. Development of this biomarker profile will provide further direction to imaging corelabs attempting to deploy ASL in clinical trials. In addition, CBF can be affected by many physiological factors, including age, gender, fasted state, caffeine intake, exercise, prescription drug and disease [42, 46-49], orsee Clement et al for a systematic review on all these effects, including handy pre-defined questionnaires to use in clinical trials[50]. To account for these variables, study groups/cohorts should be as closely matched as feasible to allow the exploration of the factors of interest, such as drug effects. Physical state of the subjects should be carefully controlled for MRI scans (e.g. no caffeine intake or strenuous activity 3 hours before MRI). Prescription drugs that may affect CBF and/or vascular tone should be excluded. Correction for partial volume effects should be considered in studies where atrophy may be present, or at least interpretation of uncorrected CBF data alongside any volumetric changes [51, 52].

Quality control of ASL imaging data

When site qualification is complete (see Appendix A for site setup and qualification recommendations, Appendix C for data storage, format and workflow) and an approval to scan first subject has been issued to a site, it is important that the imaging Core Lab continues to monitor image quality of ASL data. It is advisable to perform checks for both image quality control (image QC) and protocol adherence (technical QC) as soon as possible after a dataset has been submitted by a site. Detecting and resolving issues quickly can limit the number of affected datasets and therefore any adverse effects on downstream analysis processes. One approach taken may be to limit a site to imaging a single subject and only allowing them to proceed with imaging of further trial participants once this first dataset has passed QC criteria (for subject preparation for scanning, please see Appendix B). Imaging QC processes may be manual, semi-automated, fully-automated, or a mixture of these approaches in an effort to best detect issues in the data.
The following section describes some of the common issues and artefacts observed in ASL datasets, how they can be detected, and possible approaches to enhance data by removing errors (e.g. by modifying the acquisition parameters, or cleaning/scrubbing the acquired ASL data).

Visual QC

For all neuro ASL acquisitions and scanner generated outputs, an initial visual check for adequate brain coverage and noticeable artefacts is required. If raw ASL images are available, quick visual assessment of the images can be performed by calculating a temporal variance image. Given that perfused areas display the largest changes in signal intensity due to perfusion, the corresponding temporal variance will also display the largest variance. A variance image resembles a PWI image.

For both PWI (mean or time series) and generated CBF images, the visual image QC process can be divided into two parts: assessment of images for the presence of expected contrast between anatomical regions of the brain (contrast QC) and checks for the presence of artefacts in the images (artefact QC). If other ASL parametric maps (e.g. arterial transit time (ATT)) are generated by post processing software, these should also be assessed.

Contrast in PWI (and CBF maps) is driven by the arrival of the labeled blood bolus, and contrast between GM and WM tissue regions should be clearly visible. In cases where ASL image quality is very high, it may also be possible to observe contrast between WM and cerebrospinal fluid (CSF) regions. In some distal brain regions where the labeled blood must travel further, known as border zone or watershed regions, the ASL signal may be lower [53]. In these regions it is important to identify the cause of the lower PWI and CBF estimates, and if it is driven by longer ATT, it may be necessary to adjust the pulse sequence inflow time to account for this. If the labeling efficiency of the pulse sequence used is too low, or images have been acquired or scaled incorrectly, erroneous PWI and CBF values and poor contrast between WM and GM structures will result. For example, particularly low PWI and CBF in an entire vascular territory may indicate

a labeling failure for the artery feeding that territory. The mean CBF value for whole brain GM should fall within the range of 40-100 mL/min/100 mL [20], and GM/WM CBF ratios may be of the order of 2-2.5 [54, 55]. In GM regions, localized regions of spurious PWI and CBF values may indicate an issue, as the signal should be reasonably homogenous and vary smoothly.

Image artefacts need to be detected as part of the ASL image QC process, as resulting deviations in signal intensity may cause significant errors that propagate into the CBF maps. Checks for motion, susceptibility, and vascular artefacts should be assessed at a minimum. ASL pulse sequences are particularly sensitive to head motion, which causes blurring and a reduction in contrast between WM and GM regions. Motion issues can be identified visually as signal outside of the brain in the PWI and CBF maps that is sometimes described as a 'hyperintense rim'. Magnetic susceptibility effects on ASL data will cause signal to drop out and distort anatomy. An appearance of unnaturally shaped, region-specific areas lacking image contrast may indicate susceptibility driven artefacts. Regions of spurious signal or 'bright spots' may be indicative of vascular signal, which can be caused by an incorrect ASL inflow time used during imaging or Or prolonged ATT which may be seen more often in older subjects or some pathologies [56].

To remove reader bias and standardize contrast QC and artefact QC activities in ASL clinical trials, a scoring method was recently published [57]. This approach may be highly beneficial for increasing sensitivity to detection of poor-quality imaging data and increasing reproducibility of QC techniques in multisite ASL imaging trials.

Automated QC

In addition to the above visual QC processes, several ASL data processing strategies have been proposed for the automated detection and exclusion of artifacts in ASL data (referred to herein as "ASL scrubbing"). We broadly categorize these as either motion-based or signal-based approaches that can be further subcategorized into threshold-based or threshold-free approaches.

Because ASL is based on subtraction of temporally adjacent volumes, any relative displacement will significantly affect CBF estimation, so motion is severely detrimental for CBF measurements. Estimating motion in the ASL (control-label) timeseries using motion-based approaches allows to identify individual volumes with excessive motion that can be excluded using either. Miranda et al. proposed to reject images with more than a threshold 2 mm translation or 1.5° rotation between successive images in the ASL timeseries [58]. More conservatively, Jann et al. proposed (implemented in the CereFlow software) a frame-wise displacement (FD) threshold of > 0.8 mm for rejecting images from pCASL time series [59]. Signal-based ASL scrubbing can also be used to detect motion artifacts and other imaging artifacts. Tan et al proposed a simple yet effective PWI signal filtering approach: removing outliers from the PWI time series if the mean and standard deviation was outside a predefined threshold of the quantities across time [60]. A threshold-free

method named Enhancement of Automated Blood flow Estimates (ENABLE) sorts control-label pairs by motion and cumulatively averages them until the addition of further pairs significantly decreases the temporal voxel-wise signal stability [61]. An implementation of this technique (ExploreASL: [62]) employs the median GM voxel-wise temporal SNR (tSNR) as the criterion for signal stability , regularized by an empirically-defined minimum tSNR improvement of 5% [63].

Motion-based and signal-based strategies can also be combined for artefact detection. Wang et al. utilized head motion (both absolute motion and relative motion between each control-label pair) and global signal deviations to exclude outlier timepoints from the ASL series [64]. In further work, Wang et al. proposed an adaptive outlier cleaning approach (AOC): using the mean CBF as the reference and iteratively removing timepoints based on the degree to which they vary from the reference [49]. Outliers identified based on head motion estimations were removed before calculating the initial mean in the AOC. Similarly, Dolui et al. combined both motion-based and signal-based strategies for artefact detection; utilizing a structural correlation-based outlier rejection scheme with pre-processing to remove extreme outliers (SCORE+) to reject outliers in the CBF time series of 2D-PASL data [46].

Although these approaches help in reducing artifacts introduced into CBF calculation, every effort should be made to minimize them while acquiring the data. For example, head motion can be reduced by properly immobilizing the head for the scan (See Appendix B for subject preparation).

Quantitative analysis

The analysis of ASL data begins with pre-processing the raw images to be able to quantify them. Steps include removing nuisance images (scrubbing) and motion correction to generate perfusion-weighted images (PWI). According to the acquisition strategy, PWI are then converted to absolute CBF maps. The steps are described in detail below.

Pre-processing Steps

Typical pre-processing steps may include scrubbing, motion correction, registration, and less commonly, distortion correction. Scrubbing is already discussed in the previous QC session.

Motion correction is performed similar to other functional MRI data, i.e. to perform rigid registration between individual volumes. It is important to perform motion correction before the control and label subtraction. ASL data acquired using EPI technique with some scanners may also suffer the distortions common to all EPI-based techniques. There are two options for distortion correction: to collect a separate field map [65] or to acquire the calibration image twice with opposite phase-encode directions to the ASL data [66]. In both cases, methods are applied to reduce/correct these distortions [65, 66]. For 3D acquisitions, motion correction maybe limited as scanners only acquiring a handful of tag/control pairs, which not often are

saved, and only the resulting PWI or CBF images are saved. In such cases, motion correction provides limited or no help in reducing artifacts.

It is often needed to transform low resolution ASL data to a template space to be able to report regional statistics on CBF map. It is typically conducted in two steps: 1) registration of the M0 image or mean PWI to the high-resolution structural image (e.g. T1W) 2) registration of the structural image to a standard template space (e.g. MNI152). The GM/WM tissue probability maps resulting from these registration steps can also be used for partial volume correction and masking the volumes by GM masks.

After pre-processing, pairwise subtraction between control and label images is performed, and the average of the difference of the images gives the PWI, which is used in clinical practice. The PWI reflects the perfusion in each voxel, but the intensity value does not provide an absolute measure of perfusion.

Quantification of CBF

Under a few assumptions, the PWI can be used to quantify CBF with a simple model. For details of how these equations are derived, the reader is referred to these publications [67, 68].

For PCASL [67],

$$CBF = \frac{6000*\lambda*(SIcontrol-SIlabel)*e^{\frac{PLD}{T1,blood}}}{2*\alpha*T1,blood*SIPD*(1-e^{\frac{\tau}{T1,blood}})}[ml100g/min]$$

For QUIPSS II PASL [68],

$$CBF = \frac{6000*\lambda*(SIcontrol-SIlabel)*e^{\frac{TI}{T1,blood}}}{2*\alpha*TI1*SIPD}[ml100g/min]$$

The parameters for these equations are shown in **Box 2**. One aspect to be aware of is that usually SIPD is acquired in a different scan, intensity scaling sometimes needs to be applied in order to accurately calculate CBF, different scanner manufacturer handle the global scaling factor differently. The reader is referred to Appendix D for a description of how to apply it.

Partial Volume Effects

The spatial resolution achievable with ASL in current scanners is of the order of 2-4 mm in the plane of acquisition and 3-5 mm slice thickness. Accordingly, many voxels will consist of a mixture of grey, white, and CSF components. GM and WM have different perfusion characteristics, and CSF presents no flow determinable by ASL techniques. Compounded with this, disease and age will further alter the relative content of each component. For example, subjects with significant

brain atrophy may present reduced cortical GM and enlarged ventricles, as compared to normal and/or younger subjects. Uncorrected CBF values for partial volume effects may result in artifactual differences, if groups present different levels of atrophy.

There has been interest in properly quantifying CBF specifically in regions where these mixtures are present. Partial volume effect corrections (PVC) have been approached in a variety of forms described below. For more details and implementations, the reader is encouraged to review the cited literature.

Partial tissue volume content method

The initial and most common PVC method for ASL [69, 70] assumes a fixed ratio of CBF between GM and WM. It utilizes a high-resolution T1 image to create probability or fractional spatial maps of GM, WM, and CSF in each voxel. The low resolution CBF map is then co-registered to the high-resolution tissue segmentation and the relative contribution of each one is determined. This approach, however, is susceptible to the assumption of fixed GM/WM CBF ratios and to the errors introduced by the segmentation and registration processes [71].

Local linear regression

A local linear regression approach assumes constant CBF for GM and WM voxels within a n2 kernel around the voxel with partial volume effects using the information obtained from segmentation of anatomical image [72]. This approach produces CBF maps for GM and WM. However, it introduces significant spatial smoothing reducing the ability to resolve anatomy [52].

Spatially Regularized correction

To overcome smoothing introduced by the linear regression approach, a spatially regularized correction approach has been developed. This approach uses a formulation in which GM and WM CBF is subjected to spatial priors within a Bayesian inference scheme, which produces CBF maps that do not display the level of smoothness introduced in the linear regression approach. The method was initially developed for multi-PLD data sets [52], but it has been shown to also work with single PLD datasets [51].

Super resolution Reconstruction

All the PVC methods described above are applied in the original resolution of the acquired images. While reducing the effect of partial volume composition, they do not allow for an increase in the level of anatomical details in the image. However, super resolution (SR) reconstruction approaches allow for the correction of for partial volume effects and provide higher spatial resolution CBF maps [73].

The application of deep learning (DL) techniques to increase spatial resolution has been making significant progress across different image modalities [74], and DL methods for achieving high-resolution, high-SNR ASL have been a focus of recent research. When a large amount of training data is provided, these techniques have been widely used in ASL denoising, with great success [75-78]. A study by Zheng et al. suggested a two-stage multi-loss SR network that improves both spatial resolution and SNR of ASL scans [79]. This method, like those of other supervised DL approaches, requires a large number of high-quality ASL images for training.

Review of Existing Software

Several ASL analysis packages (and likely many more in-house scripts and pipelines) exist to aid with the processing of ASL data. For example, the aforementioned ASLtbx [64] and ExploreASL [62], as well as CereFlow [https://www.transmri.com/cereflowtm] and OxASL [https://oxasl.readthedocs.io/en/latest/]. The Open Science Initiative for Perfusion Imaging (OSIPI) inventory is a good resource for ASL pipeline inventory [https://docs.google.com/document/u/1/d/e/2PACX-1vQ-1GF2fmz6Q4IukuKP_-57H-xi872Xq_uBlX5P0Cwpj4RYd_t73pvZ64UqXegPaVpQJhQQrVRJRPro/pub]. Knowing which package to select and use for a particular study can be a daunting task and depends on many factors, such as:

- *Licensing* – Is this product licensed to use for my study? Often licensing is free for academic studies, and either not licensed or licensed with a fee for commercial use.
- *Hardware/software* – What hardware/software requirements are needed to run the ASL analysis package? Some analysis packages are limited to operating systems. (Windows/Mac/Linux), and may require a minimum CPU, hard disk storage or system memory.
- *Workstations/users* – How many workstations and users can access the analysis software at any one time? Depending on the design of the product itself and the licensing agreement, the analysis package may be for a single workstation and single user, single workstation allowing multiple users, or a floating license that can be used on numerous workstations and for multiple users. This is an importance consideration when planning study throughput.
- *Processing capability* – Can the analysis package process my ASL data and provide the outputs that I require? Some analysis packages are limited to ASL data from certain vendors (e.g., Siemens/GE/Philips), certain 'flavors' of ASL (e.g., pCASL), or single-delay ASL processing, so it is important to check for desired processing capability before engaging with a particular analysis package.
- *Regulatory status* – What regulatory clearance does the analysis package have and is it suitable for my study? For example, if ASL analysis results are to be submitted to the FDA, then a product conforming to 21 CFR Part 11 compliance will be required.

The above checklist is a proposed starting point, which should be coupled with additional consideration of the details for ASL processing itself (i.e., features such as QC, motion correction, outlier detection, modelling, and partial volume correction), as well as the accuracy and reproducibility of the outputs provided by the analysis packages.

Application of Machine Learning for Patient Classification and Disease Definition

Artificial intelligence (AI) and machine learning (ML) approaches may eventually provide automated screening platforms and assist in the diagnosis of various types of dementia. Several techniques have been developed for structural MRI scans of the brain that can show tissue loss associated with the disease [80]. However, it is known that the brain undergoes physiological changes prior to structural changes [81], such as the regional hypoperfusion in Alzheimer's Disease (AD) patients compared to healthy controls, as measured by ASL [69]. As a result, functional and ASL scans could be combined for the analysis of patient classification at an earlier disease stage. For example, Collij et al. have developed a ML approach based on ASL CBF measures to distinguish between patients with Alzheimer's disease and two early forms of dementia that can be precursors to the Alzheimer's disease, mild cognitive impairment (MCI) and subjective cognitive decline (SCD) [3]. This approach distinguishes between Alzheimer's disease and SCD with 90 % accuracy and between Alzheimer's disease and MCI with 82 % accuracy[3].

The application of DL approaches has not been investigated for ASL images. One reason DL has not yet been applied to ASL could be the challenges that researchers face in acquiring the large number of datasets required for such an application. Implementation of the guidance outlined in this review may help to fill this gap by providing robust and reproducible acquisitions in multicenter clinical trials.

Discussion

In this review, we have detailed the flexibility and utility of ASL MRI for measuring CBF. However, ASL has limitations in its application. Knowledge of these limitations and how to identify, limit, and control them, is the key to providing high quality, interpretable, and meaningful results for a study. For example, the inherently low SNR of ASL MRI is a limitation, but careful selection of ASL labeling and readout schemes can improve this. The lack of widely used ASL phantoms is also a limitation, since without phantoms the precise measurement error for a given combination of ASL sequence and system is unknown. Advances have been made in the ASL phantom, eg a phantom called Quantitative Arterial Spin Labelling Perfusion Reference (QASPER) has been made available for purchase since 2018 [https://www.goldstandardphantoms.com/products/qasper/]. Our recommendation, if possible, is to establish in-house data on baseline CBF variability (test-retest) for a particular setup on a given study. In research studies that include a control group and an experimental group who will receive an intervention or treatment that is expected to affect the measured outcome (e.g. CBF), the aforementioned test-retest data enables *a priori* calculation of the required magnitude of change to observe a target effect size and, in turn, to calculate required sample sizes[28].

When exploring the central (i.e., cerebral) effects of interventions and treatments on CBF, any undesirable peripheral cardiovascular effects also need to be considered and potentially controlled. For example, compounds that alter heart rate, blood pressure, and arterial transit time may impact the measured CBF [82], which is particularly important in single-delay ASL, since the measurement of CBF is established from a single snapshot in time. Capturing supplementary clinical data (e.g., HR, BP), or performing simulation work, can assist in evaluating these changes and interpreting CBF results [83]. Additionally, a second compound could be co-administered to block the undesirable peripheral cardiovascular effects (e.g. co-administration of low-dose the β-blocker nadolol [83-86]. In which case, assessment of any central effects of each compound individually, as well as when co-administered, is essential.

Summary

ASL allows for the quantification of CBF and its utility in clinical trials is expanding, although still is hampered by the diversity of acquisition modalities and analysis approaches currently present within the clinical market. The QIBA is leading in developing a profile for ASL, which will help researchers and clinicians adopt standards in the process of acquiring, measuring, and interpreting CBF values through ASL. In addition, the commercial availability of the prescribed sequence based on the ASL White Paper as part of the latest software packages from each of the main vendors will further reduce this heterogeneity. The lack of use of exogeneous contrast agents (e.g. gadolinium-based) and low risk associated with MRI places ASL as a promising tool for CBF measurement. As more PET radiotracers are developed to assess different mechanisms of neurodegeneration, ASL may provide a useful alternative to standard metabolic measures of blood flow obtained with FDG PET and H2(15)O PET [87], as use of ASL would reduce the radiation exposure for the subject. With improvement in MRI equipment, standardization of acquisition protocols, and development of analysis methodologies, ASL may become an important tool for assessing cerebral physiology in neurodegenerative conditions and treatments.

References

1. Sweeney MD, Kisler K, Montagne A, Toga AW, Zlokovic BV. The role of brain vasculature in neurodegenerative disorders. Nat Neurosci. 2018;21(10):1318-31.
2. Zonneveld HI, Loehrer EA, Hofman A, Niessen WJ, van der Lugt A, Krestin GP, et al. The bidirectional association between reduced cerebral blood flow and brain atrophy in the general population. J Cereb Blood Flow Metab. 2015;35(11):1882-7.
3. Collij LE, Heeman F, Kuijer JP, Ossenkoppele R, Benedictus MR, Moller C, et al. Application of Machine Learning to Arterial Spin Labeling in Mild Cognitive Impairment and Alzheimer Disease. Radiology. 2016;281(3):865-75.
4. Melzer TR, Watts R, MacAskill MR, Pearson JF, Rueger S, Pitcher TL, et al. Arterial spin labelling reveals an abnormal cerebral perfusion pattern in Parkinson's disease. Brain. 2011;134(Pt 3):845-55.

5. Vanherle L, Matuskova H, Don-Doncow N, Uhl FE, Meissner A. Improving Cerebrovascular Function to Increase Neuronal Recovery in Neurodegeneration Associated to Cardiovascular Disease. Front Cell Dev Biol. 2020;8:53.
6. Lansberg MG, Straka M, Kemp S, Mlynash M, Wechsler LR, Jovin TG, et al. MRI profile and response to endovascular reperfusion after stroke (DEFUSE 2): a prospective cohort study. Lancet Neurol. 2012;11(10):860-7.
7. Shi F, Gong X, Liu C, Zeng Q, Zhang M, Chen Z, et al. Acute Stroke: Prognostic Value of Quantitative Collateral Assessment at Perfusion CT. Radiology. 2019;290(3):760-8.
8. Wise RG, Tracey I. The role of fMRI in drug discovery. J Magn Reson Imaging. 2006;23(6):862-76.
9. Nery F, Buchanan CE, Harteveld AA, Odudu A, Bane O, Cox EF, et al. Consensus-based technical recommendations for clinical translation of renal ASL MRI. MAGMA. 2020;33(1):141-61.
10. Odudu A, Nery F, Harteveld AA, Evans RG, Pendse D, Buchanan CE, et al. Arterial spin labelling MRI to measure renal perfusion: a systematic review and statement paper. Nephrol Dial Transplant. 2018;33(suppl_2):ii15-ii21.
11. Telischak NA, Detre JA, Zaharchuk G. Arterial spin labeling MRI: clinical applications in the brain. J Magn Reson Imaging. 2015;41(5):1165-80.
12. Petcharunpaisan S, Ramalho J, Castillo M. Arterial spin labeling in neuroimaging. World J Radiol. 2010;2(10):384-98.
13. Williams DS, Detre JA, Leigh JS, Koretsky AP. Magnetic resonance imaging of perfusion using spin inversion of arterial water. Proc Natl Acad Sci U S A. 1992;89(1):212-6.
14. Chappell MA, MacIntosh BJ, Okell TW. Introduction to Perfusion Quantification using Arterial Spin Labelling. Jenkinson M, Chappell MA, editors: Oxford University Press; 2017. 156 p.
15. Detre JA, Zhang W, Roberts DA, Silva AC, Williams DS, Grandis DJ, et al. Tissue specific perfusion imaging using arterial spin labeling. NMR Biomed. 1994;7(1-2):75-82.
16. Buckfield PM, Clarkson JE, Herbison GP. Sex specific growth centiles at 28-42 weeks gestation New Zealand European infants. N Z Med J. 1982;95(715):615-7.
17. Eapen LJ, Gerig LH, Catton GE, Danjoux CE, Girard A. Impact of local radiation in the management of salivary gland carcinomas. Head Neck Surg. 1988;10(4):239-45.
18. Vogelfanger IJ, Beattie WG, Brown FN, King D, Michalchuk AW, Moghal AK, et al. Secretory responses of transplanted gastric fundic pouches to psychic stimulation. Surgery. 1968;64(4):763-8.
19. Wintermark M, Fischbein NJ, Smith WS, Ko NU, Quist M, Dillon WP. Accuracy of dynamic perfusion CT with deconvolution in detecting acute hemispheric stroke. AJNR Am J Neuroradiol. 2005;26(1):104-12.
20. Alsop DC, Detre JA, Golay X, Gunther M, Hendrikse J, Hernandez-Garcia L, et al. Recommended implementation of arterial spin-labeled perfusion MRI for clinical applications: A consensus of the ISMRM perfusion study group and the European consortium for ASL in dementia. Magn Reson Med. 2015;73(1):102-16.
21. Jezzard P, Chappell MA, Okell TW. Arterial spin labeling for the measurement of cerebral perfusion and angiography. J Cereb Blood Flow Metab. 2018;38(4):603-26.
22. Ye FQ, Frank JA, Weinberger DR, McLaughlin AC. Noise reduction in 3D perfusion imaging by attenuating the static signal in arterial spin tagging (ASSIST). Magn Reson Med. 2000;44(1):92-100.
23. Vidorreta M, Wang Z, Rodriguez I, Pastor MA, Detre JA, Fernandez-Seara MA. Comparison of 2D and 3D single-shot ASL perfusion fMRI sequences. Neuroimage. 2013;66:662-71.
24. Feinberg D, Ramanna S, Gunther M, editors. Evaluation of New ASL 3D GRASE Sequences Using Parallel Imaging, Segmented and Interleaved K-Space at 3T with 12- And 32-Channel Coils. ISMRM; 2009. Honolulu.
25. Fernandez-Seara MA, Wang Z, Wang J, Rao HY, Guenther M, Feinberg DA, et al. Continuous arterial spin labeling perfusion measurements using single shot 3D GRASE at 3 T. Magn Reson Med. 2005;54(5):1241-7.

26. Gunther M, Oshio K, Feinberg DA. Single-shot 3D imaging techniques improve arterial spin labeling perfusion measurements. Magn Reson Med. 2005;54(2):491-8.
27. Chen Y, Wang DJ, Detre JA. Test-retest reliability of arterial spin labeling with common labeling strategies. J Magn Reson Imaging. 2011;33(4):940-9.
28. Ssali T, Anazodo UC, Narciso L, Liu L, Jesso S, Richardson L, et al. Sensitivity of Arterial Spin Labeling for Characterization of Longitudinal Perfusion Changes in Frontotemporal Dementia and Related Disorders. Neuroimage Clin. 2021;35:102853.
29. Petersen ET, Mouridsen K, Golay X, all named co-authors of the Qt-rs. The QUASAR reproducibility study, Part II: Results from a multi-center Arterial Spin Labeling test-retest study. Neuroimage. 2010;49(1):104-13.
30. Kilroy E, Apostolova L, Liu C, Yan L, Ringman J, Wang DJ. Reliability of two-dimensional and three-dimensional pseudo-continuous arterial spin labeling perfusion MRI in elderly populations: comparison with 15O-water positron emission tomography. J Magn Reson Imaging. 2014;39(4):931-9.
31. Hodkinson DJ, Krause K, Khawaja N, Renton TF, Huggins JP, Vennart W, et al. Quantifying the test-retest reliability of cerebral blood flow measurements in a clinical model of on-going post-surgical pain: A study using pseudo-continuous arterial spin labelling. Neuroimage Clin. 2013;3:301-10.
32. Liu M, Chen Z, Ma L. Test-retest reliability of perfusion of the precentral cortex and precentral subcortical white matter on three-dimensional pseudo-continuous arterial spin labeling. J Int Med Res. 2018;46(9):3788-95.
33. Jann K, Shao X, Ma SJ, Cen SY, D'Orazio L, Barisano G, et al. Evaluation of Cerebral Blood Flow Measured by 3D PCASL as Biomarker of Vascular Cognitive Impairment and Dementia (VCID) in a Cohort of Elderly Latinx Subjects at Risk of Small Vessel Disease. Front Neurosci. 2021;15:627627.
34. Cohen AD, Agarwal M, Jagra AS, Nencka AS, Meier TB, Lebel RM, et al. Longitudinal Reproducibility of MR Perfusion Using 3D Pseudocontinuous Arterial Spin Labeling With Hadamard-Encoded Multiple Postlabeling Delays. J Magn Reson Imaging. 2020;51(6):1846-53.
35. Binnie LR, Pauls MMH, Benjamin P, Dhillon MK, Betteridge S, Clarke B, et al. Test-retest reliability of arterial spin labelling for cerebral blood flow in older adults with small vessel disease. Transl Stroke Res. 2022;13(4):583-94.
36. Perfusion by Arterial Spin Labelling Following Single Dose Tadalafil in Small Vessel Disease (PASTIS) Trial. ClinicalTrials.gov identifier: NCT02450253. https://clinicaltrials.gov/ct2/show/NCT02450253 Updated August 21, 2018. Accessed July 26, 2022. .
37. Wang Y, Zhou L, Udayakumar D, Madhuranthakam AJ, editors. Reproducibility and repeatability of quantitative pCASL measurements in a 3D-printed perfusion phantom. ISMRM & SMRT Annual Meeting & Exhibition; 2021.
38. Mutsaerts HJ, Steketee RM, Heijtel DF, Kuijer JP, van Osch MJ, Majoie CB, et al. Reproducibility of pharmacological ASL using sequences from different vendors: implications for multicenter drug studies. MAGMA. 2015;28(5):427-36.
39. Mutsaerts HJ, van Osch MJ, Zelaya FO, Wang DJ, Nordhoy W, Wang Y, et al. Multi-vendor reliability of arterial spin labeling perfusion MRI using a near-identical sequence: implications for multi-center studies. Neuroimage. 2015;113:143-52.
40. Havsteen I, Damm Nybing J, Christensen H, Christensen AF. Arterial spin labeling: a technical overview. Acta Radiol. 2018;59(10):1232-8.
41. Pollock JM, Tan H, Kraft RA, Whitlow CT, Burdette JH, Maldjian JA. Arterial spin-labeled MR perfusion imaging: clinical applications. Magn Reson Imaging Clin N Am. 2009;17(2):315-38.
42. Baas KPA, Petr J, Kuijer JPA, Nederveen AJ, Mutsaerts H, van de Ven KCC. Effects of Acquisition Parameter Modifications and Field Strength on the Reproducibility of Brain Perfusion Measurements Using Arterial Spin-Labeling. AJNR Am J Neuroradiol. 2021;42(1):109-15.

43. Gevers S, van Osch MJ, Bokkers RP, Kies DA, Teeuwisse WM, Majoie CB, et al. Intra- and multicenter reproducibility of pulsed, continuous and pseudo-continuous arterial spin labeling methods for measuring cerebral perfusion. J Cereb Blood Flow Metab. 2011;31(8):1706-15.
44. Tanaka Y, Inoue Y, Abe Y, Miyatake H, Hata H. Reliability of 3D arterial spin labeling MR perfusion measurements: The effects of imaging parameters, scanner model, and field strength. Clin Imaging. 2018;52:23-7.
45. Golay X. The long and winding road to translation for imaging biomarker development: the case for arterial spin labelling (ASL). Eur Radiol Exp. 2017;1(1):3.
46. Dolui S, Vidorreta M, Wang Z, Nasrallah IM, Alavi A, Wolk DA, et al. Comparison of PASL, PCASL, and background-suppressed 3D PCASL in mild cognitive impairment. Hum Brain Mapp. 2017;38(10):5260-73.
47. Gonzalez JE, Stelly SP, Cooke WH. Influence of Acute Fasting on Cerebrovascular Reactivity During Mental Stress. FASEB. 2020;34(S1):1.
48. Liu Y, Zhu X, Feinberg D, Guenther M, Gregori J, Weiner MW, et al. Arterial spin labeling MRI study of age and gender effects on brain perfusion hemodynamics. Magn Reson Med. 2012;68(3):912-22.
49. Wang Z, Das SR, Xie SX, Arnold SE, Detre JA, Wolk DA, et al. Arterial spin labeled MRI in prodromal Alzheimer's disease: A multi-site study. Neuroimage Clin. 2013;2:630-6.
50. Clement P, Mutsaerts HJ, Vaclavu L, Ghariq E, Pizzini FB, Smits M, et al. Variability of physiological brain perfusion in healthy subjects - A systematic review of modifiers. Considerations for multi-center ASL studies. J Cereb Blood Flow Metab. 2018;38(9):1418-37.
51. Zhao MY, Mezue M, Segerdahl AR, Okell TW, Tracey I, Xiao Y, et al. A systematic study of the sensitivity of partial volume correction methods for the quantification of perfusion from pseudo-continuous arterial spin labeling MRI. Neuroimage. 2017;162:384-97.
52. Chappell MA, Groves AR, MacIntosh BJ, Donahue MJ, Jezzard P, Woolrich MW. Partial volume correction of multiple inversion time arterial spin labeling MRI data. Magn Reson Med. 2011;65(4):1173-83.
53. Hendrikse J, Petersen ET, van Laar PJ, Golay X. Cerebral border zones between distal end branches of intracranial arteries: MR imaging. Radiology. 2008;246(2):572-80.
54. Ostergaard L, Chesler DA, Weisskoff RM, Sorensen AG, Rosen BR. Modeling cerebral blood flow and flow heterogeneity from magnetic resonance residue data. J Cereb Blood Flow Metab. 1999;19(6):690-9.
55. Parkes LM, Rashid W, Chard DT, Tofts PS. Normal cerebral perfusion measurements using arterial spin labeling: reproducibility, stability, and age and gender effects. Magn Reson Med. 2004;51(4):736-43.
56. Deibler AR, Pollock JM, Kraft RA, Tan H, Burdette JH, Maldjian JA. Arterial spin-labeling in routine clinical practice, part 1: technique and artifacts. AJNR Am J Neuroradiol. 2008;29(7):1228-34.
57. Fallatah SM, Pizzini FB, Gomez-Anson B, Magerkurth J, De Vita E, Bisdas S, et al. A visual quality control scale for clinical arterial spin labeling images. Eur Radiol Exp. 2018;2(1):45.
58. Miranda MJ, Olofsson K, Sidaros K. Noninvasive measurements of regional cerebral perfusion in preterm and term neonates by magnetic resonance arterial spin labeling. Pediatr Res. 2006;60(3):359-63.
59. Jann K, Smith RX, Rios Piedra EA, Dapretto M, Wang DJ. Noise Reduction in Arterial Spin Labeling Based Functional Connectivity Using Nuisance Variables. Front Neurosci. 2016;10:371.
60. Tan H, Maldjian JA, Pollock JM, Burdette JH, Yang LY, Deibler AR, et al. A fast, effective filtering method for improving clinical pulsed arterial spin labeling MRI. J Magn Reson Imaging. 2009;29(5):1134-9.
61. Shirzadi Z, Crane DE, Robertson AD, Maralani PJ, Aviv RI, Chappell MA, et al. Automated removal of spurious intermediate cerebral blood flow volumes improves image quality among older patients: A clinical arterial spin labeling investigation. J Magn Reson Imaging. 2015;42(5):1377-85.

62. Mutsaerts H, Petr J, Groot P, Vandemaele P, Ingala S, Robertson AD, et al. ExploreASL: an image processing pipeline for multi-center ASL perfusion MRI studies. bioRxiv. 2019:845842.
63. Shirzadi Z, Stefanovic B, Chappell MA, Ramirez J, Schwindt G, Masellis M, et al. Enhancement of automated blood flow estimates (ENABLE) from arterial spin-labeled MRI. J Magn Reson Imaging. 2018;47(3):647-55.
64. Wang Z, Aguirre GK, Rao H, Wang J, Fernandez-Seara MA, Childress AR, et al. Empirical optimization of ASL data analysis using an ASL data processing toolbox: ASLtbx. Magn Reson Imaging. 2008;26(2):261-9.
65. Jezzard P, Balaban RS. Correction for geometric distortion in echo planar images from B0 field variations. Magn Reson Med. 1995;34(1):65-73.
66. Andersson JL, Skare S, Ashburner J. How to correct susceptibility distortions in spin-echo echo-planar images: application to diffusion tensor imaging. Neuroimage. 2003;20(2):870-88.
67. Buxton RB, Frank LR, Wong EC, Siewert B, Warach S, Edelman RR. A general kinetic model for quantitative perfusion imaging with arterial spin labeling. Magn Reson Med. 1998;40(3):383-96.
68. Wong EC, Buxton RB, Frank LR. Quantitative imaging of perfusion using a single subtraction (QUIPSS and QUIPSS II). Magn Reson Med. 1998;39(5):702-8.
69. Du AT, Jahng GH, Hayasaka S, Kramer JH, Rosen HJ, Gorno-Tempini ML, et al. Hypoperfusion in frontotemporal dementia and Alzheimer disease by arterial spin labeling MRI. Neurology. 2006;67(7):1215-20.
70. Johnson NA, Jahng GH, Weiner MW, Miller BL, Chui HC, Jagust WJ, et al. Pattern of cerebral hypoperfusion in Alzheimer disease and mild cognitive impairment measured with arterial spin-labeling MR imaging: initial experience. Radiology. 2005;234(3):851-9.
71. Ahlgren A, Wirestam R, Petersen ET, Stahlberg F, Knutsson L. Partial volume correction of brain perfusion estimates using the inherent signal data of time-resolved arterial spin labeling. NMR Biomed. 2014;27(9):1112-22.
72. Asllani I, Borogovac A, Brown TR. Regression algorithm correcting for partial volume effects in arterial spin labeling MRI. Magn Reson Med. 2008;60(6):1362-71.
73. Shou Q, Shao X, Wang DJJ. Super-Resolution Arterial Spin Labeling Using Slice-Dithered Enhanced Resolution and Simultaneous Multi-Slice Acquisition. Front Neurosci. 2021;15:737525.
74. Isaac J, Kulkarni R, editors. Super resolution techniques for medical image processing. International Conference on Technologies for Sustainable Development (ICTSD); 2015.
75. Gong K, Han P, El Fakhri G, Ma C, Li Q. Arterial spin labeling MR image denoising and reconstruction using unsupervised deep learning. NMR Biomed. 2019:e4224.
76. Kim KH, Choi SH, Park SH. Improving Arterial Spin Labeling by Using Deep Learning. Radiology. 2018;287(2):658-66.
77. Ulas C, Tetteh G, Kaczmarz S, Preibisch C, Menze BH. DeepASL: Kinetic Model Incorporated Loss for Denoising Arterial Spin Labeled MRI via Deep Residual Learning. Medical Image Computing and Computer Assisted Intervention: Springer International Publishing; 2018. p. 30-8.
78. Xie D, Li Y, Yang H, Bai L, Wang T, Zhou F, et al. Denoising arterial spin labeling perfusion MRI with deep machine learning. Magn Reson Imaging. 2020;68:95-105.
79. Li Z, Liu Q, Li Y, Ge Q, Shang Y, Song D, et al. A two-stage multi-loss super-resolution network for arterial spin labeling magnetic resonance imaging. International Conference on Medical Image Computing and Computer-Assisted Intervention: Springer, Cham.; 2019. p. 12-20.
80. Zhang Z, Li G, Xu Y, Tang X. Application of Artificial Intelligence in the MRI Classification Task of Human Brain Neurological and Psychiatric Diseases: A Scoping Review. Diagnostics (Basel). 2021;11(8).
81. Jack CR, Jr., Knopman DS, Jagust WJ, Shaw LM, Aisen PS, Weiner MW, et al. Hypothetical model of dynamic biomarkers of the Alzheimer's pathological cascade. Lancet Neurol. 2010;9(1):119-28.

82. Xing CY, Tarumi T, Meijers RL, Turner M, Repshas J, Xiong L, et al. Arterial Pressure, Heart Rate, and Cerebral Hemodynamics Across the Adult Life Span. Hypertension. 2017;69(4):712-20.
83. Bishop CA, Rizzo G, Lodeweyckx T, Hoon JD, Laere KV, Koole M, et al., editors. Disentangling apparent discordance between ASL-MRI and [18F]-FDG PET following a single dose of the β2-agonist clenbuterol. Joint Annual Meeting ISMRM-ESMRMB & ISMRT 31st Annual Meeting; 2022 May 01-12, 2022; London, England, UK.
84. Lodeweyckx T, Hoon JD, Laere KV, Koole M, Vandenberghe W, Bishop C, et al., editors. Safety, Tolerability and Cerebral Blood Flow After Single Doses of the β2-agonist, Clenbuterol, in Patients with Mild Cognitive Impairment or Parkinson's Disease. Clinical Trials on Alzheimer's Disease Scientific Committee; 2021.
85. Bishop CA, Lodeweyckx T, Hoon JD, Laere KV, Koole M, Vandenberghe W, et al., editors. Dose-dependent response of cerebral blood flow in healthy volunteers following administration of β2-adrenergic receptor agonist clenbuterol. Joint Annual Meeting ISMRM-ESMRMB & ISMRT 31st Annual Meeting; 2022 May 07-12, 2022; London, England, UK.
86. Vargas G, Bishop CA, Rizzo G, Almuqbel M, Keenan R, Rabiner E, et al., editors. Beta-Adrenoceptor Agonism Evokes Acute Imaging Signals in Healthy Individuals. The 15th International Conference on Alzheimer's and Parkinson's Diseases and related neurological disorders, AD/PD; 2021 March 2021; Virtual Conference.
87. Matthew E, Andreason P, Carson RE, Herscovitch P, Pettigrew K, Cohen R, et al. Reproducibility of resting cerebral blood flow measurements with H2(15)O positron emission tomography in humans. J Cereb Blood Flow Metab. 1993;13(5):748-54.
88. Gabrielyan M, Tisdall MD, Kammer C, Higgins C, Arratia PE, Detre JA. A perfusion phantom for ASL MRI based on impinging jets. Magn Reson Med. 2021;86(2):1145-58.

Acknowledgements and Funding

Authors Xue Wang, Courtney Bishop, James O'Callaghan, Justin Albani, Wendy Theriault, and Lino Becerra are employees of Invicro, and this publication was supported by Invicro. The authors would like to thank Dr. Kristen E. Murfin (Invicro, New Haven, CT) for providing medical writing support. Dr. Danny Wang is a share-holder of Translational MRI LLC that developed Cereflow software.

Additional Materials

Boxes, Tables, and Figures

Box 1: Main Imaging techniques for measuring brain perfusion (for Clinical Research)

	ASL	FDG PET	DSC
Contrast	None (Endogenous contrast)	Radioisotope	Gadolinium-based contrast
Spatial resolution	2-4 mm (in plane) and 4 mm (slice thickness)	4-6 mm	2 mm
Radiation	None	Yes	None
Acquisition time	5-10min	5-10min (plus uptake time)	2 min
Assessed parameters	CBF, ATT	glucose metabolism	CBV, CBF, MTT
Limitations	May require a separate license/agreement for certain ASL sequences More efforts on standardization needed (A variety of ASL sequences available)	Radiation dose limit per year Tracer dose logistics (Tracer needs to be used with certain time to avoid decay in radioactivity)	May have acute adverse reactions to the contrast agent and potential long-term gadolinium retention in brain May affect accuracy of other scans following the gadolinium injection
Subject selection		Not for pediatric subject	Not for subjects with history of previous contrast reaction, asthma, renal problems
Patient Preparation	Avoid caffeine and drugs that affect perfusion	Fasting 4-6 hours prior to scan to reduce glucose level	

Key: CBF(V): Cerebral Blood Flow (Volume); MTT: Mean Transit Time

Box 2: Parameters for the Calculation of CBF

Parameters	Value	Notes
λ (blood-brain partition coefficient)	0.9 ml/g	

T1,blood	3 T/1.5 T: 1650/1350 ms	
SI control-SI label	Average signal intensity in control-label subtraction, i.e. PWI	If the order of control-label is wrong, the perfusion value will be negative.
SI PD	Intensity in PD image	When acquired separately from the control /label scan, rescaling is needed for accurate quantification.
TI (Inversion time)		For 2D multi-slice acquisition, the value of TI needs to be adjusted for each slice to take into account the time delay between slices. No need for 3D acquisition.
α (labeling efficiency)	PCASL: 0.85; PASL:0.98	
Background suppression efficiency	GE 3D spiral:0.75 (Garcia et al., MRM 2005) Philips 2D EPI or Siemens 3D GRASE :0.83 Philips 3D GRASE:0.81	When background suppression is applied, the overall efficiency is a combination of both inversion efficiency and background suppression efficiency.
PCASL, PLD (post labeling delay)		Extract from the DICOM header/protocol, for details please refer to the appendix. For multiple PLD sequences there will be multiple PLD values.
PASL TI1, TI		
□ (tau)	Label duration	

Table 2. ASL pulse sequence recommendations

Imaging recommendations		*Labeling recommendations*	
Parameter name	Preferred value	Parameter name	Preferred value
2D or 3D	3D	PASL or PCASL	PCASL
TR	Minimum possible for given labelling parameters.	PCASL labelling duration	1800 ms
FOV	220 mm (full FOV required, no rectangular FOV) Coverage of whole brain in slice direction	PCASL PLD	1500 ms – 2000 ms
Resolution	3.4 mm×3.4 mm in plane 4.0 mm slice	PCASL Average labelling gradient	1mT/m
Flip angle	90	PCASL slice select gradient	10mT/m
Field strength	1.5 T or 3 T (3 T preferred)	PASL TI1 (QUIPSS II Saturation Time)	800 ms
TE	Minimum allowed	PASL Labeling Slab Thickness	15-20 cm
Imaging sequence	3D GRASE or 3D Stack of spirals (2D EPI acceptable)	Time-encoded PCASL	Off
Acquisition plane	Scanner Axial / Transverse		
Phase encode	A-P or P-A (3D GRASE and EPI)		
Acquisition readout	4 – 15 ms readouts, turbo-factor of 8 to 12; echo train of up to 300 ms (3D RARE or GRASE) Single shot, minimum echo time (EPI)		

Scan time	Approximately 5 minutes.	

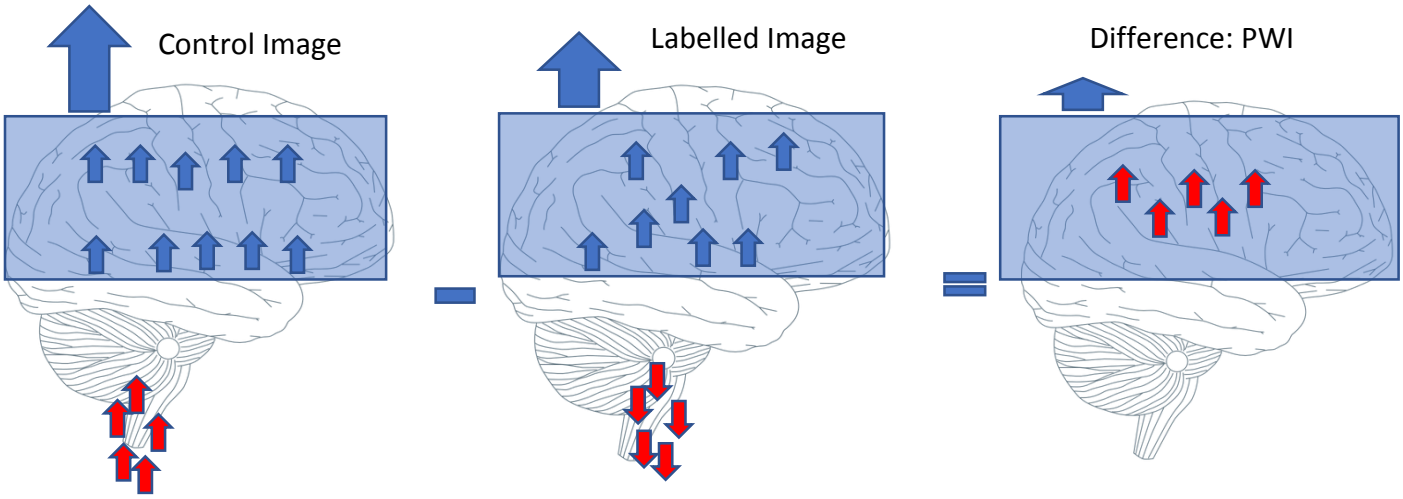

Figure 1: ASL mechanism. The difference(right) between the control (left) and labeled (middle) image determines the ASL. In the labeled images, blood water protons (red arrows) outside of the imaging volume (blue box) are labelled by magnetic inversion (negative magnetization). After a period of time, generally referred to as the 'inflow time', the image acquisition commences. The inflow time is long enough so that the labeled blood water flows into the imaging volume and mixes with the (positively magnetized) static tissue water in the parenchyma (blue arrows in within the blue box). This results in a net reduction of the parenchymal MRI signal in this 'labelled' image. A relative measure of perfusion can be calculated by acquiring an unlabeled (control) image (note that in control image the blood water protons are not inverted) and calculating the signal difference compared to the labeled image. The static tissue signal from control and labeled image will be cancelled in the difference image, and the net difference is related to cerebral blood flow.

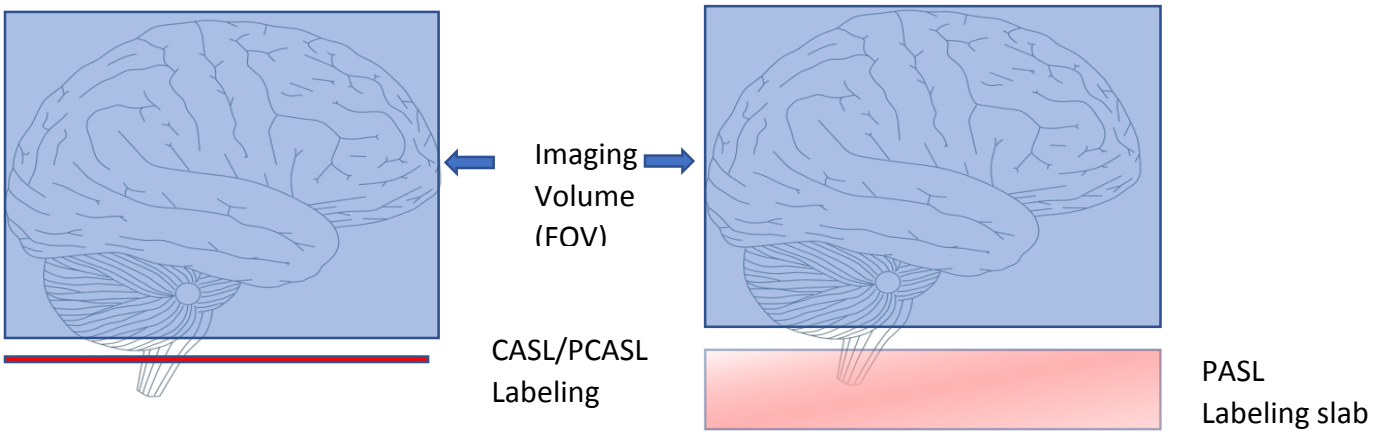

Figure 2: The two most common labelling approaches for ASL are pseudo-continuous ASL (PCASL) and pulsed ASL (PASL). For PCASL, many RF pulses are applied in rapid succession (over the order of milliseconds) and for a relatively long overall duration (1-3 seconds), to invert and label arterial blood water as it flows through a relatively thin labelling plane (on the left). In contrast, PASL typically uses a single RF pulse applied for a much shorter total duration (e.g. 10–20 ms), to simultaneously invert arterial water in a thick labelling slab (on the right).

Supplementary Data

Appendix A: Imaging site setup and qualification

Prior to participating in a clinical trial, candidate imaging centers should be provided with appropriate training and then be evaluated to ensure they will be able to perform activities as required by the study protocol. The site setup process may be carried out by an imaging corelab, coordinating and working with potential imaging sites, and can include the steps shown in **Figure 3**. The setup is initiated though a request to the site for information on their equipment and expertise. The corelab will then train the site to perform imaging services as required for the ASL study. When the corelab has reviewed all material provided by the site and found it to be compliant with the trial protocol, the qualification process ends, and the imaging center will be accepted onto the ASL clinical trial.

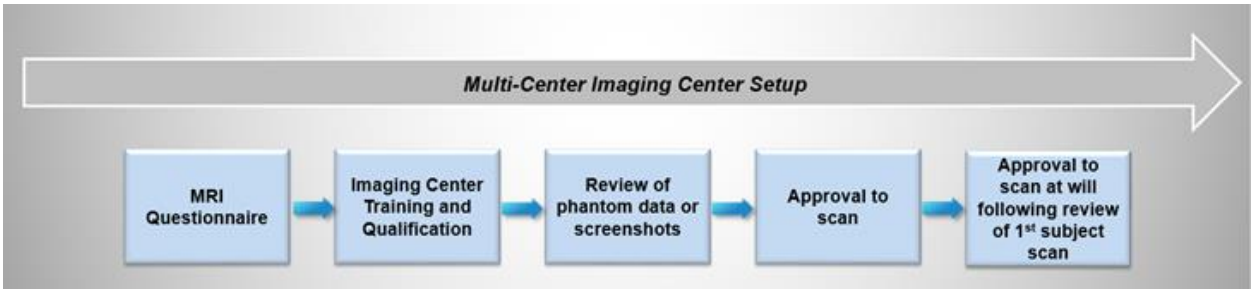

Figure 3: Flow diagram depicting main imaging site setup activities involved in a multi-center clinical trial.

To ensure high quality ASL data, a standardized imaging protocol must be developed for the trial and deployed consistently across imaging sites (see Image Acquisition in the main text for recommendations). Requirements for imaging equipment and staff expertise will be identified by the imaging corelab to ensure that it will be possible for the multicenter imaging protocol to be implemented at candidate sites. Relevant information will be provided by imaging centers and captured in a document such as a site questionnaire. In addition to identification and contact details, it is advised that the site questionnaire includes details regarding experience of trial-specific imaging, all staff that will take part, data transfer experience, imaging hardware and pulse sequences available, and details of their MRI quality control and maintenance activity.

The suitability of MRI scanning equipment at each site will be evaluated for inclusion on the clinical trial based on information provided in the site questionnaire. For ASL studies, a field strength of 3 T is preferred, although 1.5 T may be considered, depending on the trial requirements. Sites will be asked to supply details for multiple scanners at their imaging center so that a secondary scanner can also be qualified for situations where the primary scanner is unavailable (any planned upgrades/purchases/decommissions should be captured in the

questionnaire). Finally, details of radio frequency coil hardware, scanner software version and access to pulse sequences listed in the trial protocol should be confirmed.

To ensure satisfactory performance, it is important that MRI scanners have regular preventative maintenance visits and are monitored as part of a local QA program. In addition to these activities, the imaging corelab will assess technical scanner performance using multicenter phantom QC protocols. It will be necessary to assess image quality metrics of signal-to-noise ratio, signal uniformity, and geometric distortion, at a minimum, and there should also be visual checks for image artifacts. If system performance is satisfactory, the full ASL imaging protocol should be acquired in a phantom. ASL phantoms have recently become available that contain chambers of flowing fluid in which perfusion measurements can be made [88]. These phantoms may add value by allowing enhanced site QC of ASL MRI sequences as they become more readily available. A technical QC of acquisition parameters should be carried out on all data submitted by sites to ensure that the protocol was implemented as specified. It may take multiple iterations, with additional support and training from the corelab, before a site meets all image and technical QC criteria and is given approval to scan the first trial subject.

Appendix B: Patient Preparation

Instruction should begin with subject scheduling; in advance of arrival, subjects should be informed of the exam details. Additionally, subjects should be reminded to avoid caffeine 1 hour prior to the exam and avoid gadolinium-based contrast agents within 48 hours of the exam. Finally, a thorough screening for any contraindications should be reviewed with the subject.
Upon arrival to the imaging center, the subject's history should be reviewed again to ensure that it is safe for the patient to undergo the MRI. The exam should again be thoroughly explained to the subject, so they know what to expect, especially regarding the noise and length of time. Reassure them that the magnet is open on both ends and that you can always see and hear them and provide a squeeze ball to be used in case the subject has a problem. Have the patient change out of their clothes into a metal free gown, and ensure that all jewelry, hair accessories, and eye make-up has been removed.

Place the patient supine with their head resting comfortably in the head coil. Ensure that the head is in a neutral position, avoiding flexion or extension of the head and without a right or left head tilt. The subject's head should be completely within the head coil so that there is no signal drop off inferiorly and not pushed in so far that the signal drops off superiorly. Secure the head with immobilizing devices such as foam padding and/or the paddles from the head coil. This is very important, as head motion severely affects CBF measurements. Center the nasion to the center of the head coil and then center the laser to the center of the head coil. Ensure that the head coil is pulled completely forward or down. This series is sensitive to motion and extra care should be taken to make patient comfortable and immobilized.

Once the patient is positioned, perform a 3 plane scout. Review the scout to ensure that the signal is homogenous, no artifacts from metal are seen, and that the patients head is straight. Re-position the subject if necessary. Once the scout is acceptable, prescribe a sagittal T1 weighted image to further localize. Again, assess the sagittal image for quality and window appropriately to visualize the brain anatomy, and prescribe the Imaging Volume (slab) axially from the midline of the T1 sagittal series, including the brain in its entirety from inferior posterior fossa to 1 slice above the vertex of skull. There should be no brain tissue on the most superior slice. This volume should not be angled. Place the labeling plane inferior and parallel to the Imaging volume at the level of C1, Place the labeling slab inferior to the labeling plane which should also be parallel to the imaging volume.

The slices should be centered in the axial plane to prevent aliasing in the Anterior/Posterior direction.

Prior to starting the scan, the patient should be instructed to keep their eyes open during the entire series. Ask them to focus on a point on the head coil or mirror if the head coil is equipped with one. There can be no external stimuli from an audio/visual source, meaning the patient cannot listen to music or watch a movie during this series. When the scan is finished, verify with the patient that they kept their eyes open and did not fall asleep. Check the images for motion or other artifacts, and ensure all slices were reconstructed prior to having the subject leave. Repeat if necessary and if the patient will allow. If the patient moves to sit up or use the restroom, a new localizer (scout) is necessary.

Appendix C: Data storage, Data format, workflow

How the ASL data will be collected and curated is essential for maintaining high-quality standards, and details of data collection and curation should be decided on prior to study subject imaging. The software platforms to be used, ancillary information to be collected, methods for data collection, data de-identification and naming conventions, file format, and data transfer pathway(s) are essential points to consider for study data management. When making these operational decisions, it is imperative to ensure adherence to all applicable regulatory requirements, which will vary based on the phase of the trial and objectives for the ASL component. In addition, as multiple groups (e.g. sponsor, imaging center(s), clinical site(s), imaging contract research organizations (CROs), and/or clinical CROs, etc.) are routinely involved with various aspects of the trial, it is important to take into account the particular needs of each group when considering trial data management elements to allow for efficient analysis and reporting of results.

Web-based data management platforms have become the standard for transferring image files, capturing applicable metadata relevant to the imaging procedure for later use in analysis and reporting, and supporting custom image processing workflows. Through electronic data

management platforms, image files and scan metadata are able to be uploaded by the imaging center personnel to the processing group, which allows for a variety of potential manual and automated steps for data quality control, query resolution, analysis, and storage. Web-based data management portals may also integrate electronic query resolution capabilities for managing discrepancies found as part of quality control or analysis, facilitating accelerated resolution of queries for fast-paced trials utilizing ASL as a decision-making tool for dose escalation, cohort assignment, etc.

As displayed in **Figure 4**, study-specific processing workflows may be utilized to incorporate functionality such as programmed conformity checks for prevention of data entry discrepancies, automated file anonymization and conversion to standardized format, quality control steps assessing adherence to defined acquisition protocols, and automated pre-processing and analysis steps. Such workflows may incorporate what is commonly termed Business Process Modeling (BPM) along with system integrated workflow engines to efficiently and programmatically complete specific processing tasks, which reduces the need for manual steps while notifying users when manual intervention is required. An example workflow incorporating independent container applications, executing automated processing algorithms, integrated with manual intervention checkpoints for the review of results between sequential automated analysis steps, is displayed in **Figure 5**.

Data management platforms also enable the implementation of user-specific access controls for analysis. Metadata forms and database access can be restricted to designated personnel, with assignment of internal codes for image files, removing visibility to information such as clinical data and dosing cohort assignment, which may bias an analyst and result reporting.

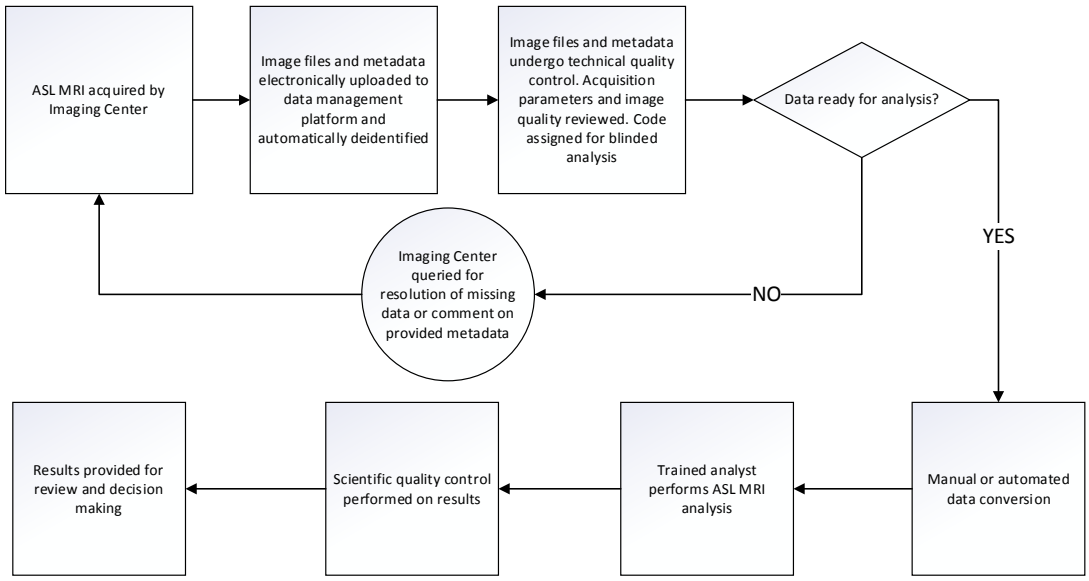

Figure 4: Example Study-specific Processing Workflow

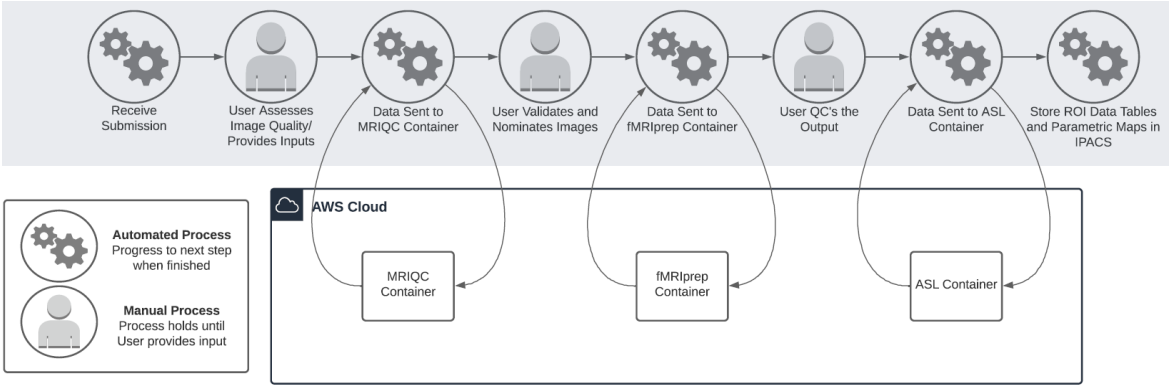

Figure 5: Example Workflow with Independent Container Applications

Appendix D: Global scaling difference between the ASL data and the calibration image

The image intensity in the calibration image is usually much higher than the label/control image. To increase the accuracy, a different gain setting might be used for the ASL data and the calibration image, if acquired separately. In this case, a global scaling factor needs to be applied to make the ASL data and calibration image intensity match to be able to get accurate perfusion values.

For Siemens, the calibration image needs to be divided by 10.

For GE 3DASL, the default scaling factor is 32 for PWI and stored in the PWI header (0043,107F) 2nd value. GE accumulates signal instead averaging by NEX, therefore PWI images needs to be divided by the Number of average (NEX: number of excitations).
Some older GE systems may have limitations eg images are stored in12-bit data limit additional steps are needed to correct the image intensity.

Unlike GE and Siemens, Philips image intensity has a scaling factor (ref https://www.ncbi.nlm.nih.gov/pmc/articles/PMC3998685/). Relationships between the original pixel floating-point (FP) value, stored Precise Value (PV), Rescale Intercept (RI), Rescale slope (RS), scale slope (SS), scale intercept (SI), and display value (DV) are documented in text headers of Philips PARameter/REConstructed image file formats. These parameters are also available in public tags of Philips MR DICOM: RI in address [0028,1052] and RS in [0028,1053]; and in private tags: SI in [2005,100D] and SS in [2005,100E]. Relationships between image-scaling parameters are
FP=(PV-SI)/SS

Depending on the dicom to nifti conversion software/version/option used, the nifti image intensity may need to be rescaled to reflect the correct FP.